Progress In Electromagnetics Research B, Vol. 51, 329–346, 2013

WIRELESS COMMUNICATIONS IN A TREE CANOPY

Pobsook Sooksumrarn, Chainarong Kittiyanpunya, Paiboon Yoiyod, and Monai Krairiksh*

Faculty of Engineering, King Mongkut's Institute of Technology Ladkrabang, Thailand

Abstract—The wireless communications in a tree canopy is essential for pre-harvesting control of fruit productions. To efficiently communicate between a sensor node and a sink node, channel characteristics in a tree canopy must be well-established. In this paper, propagation channel characteristics at the frequencies of 2.45 and 5.2 GHz have been estimated for designing a wireless communication system in a tree canopy. The proposed solution is based on measured path loss, time-varying signal strength and Angle of Arrival (AoA) for various paths in a tree canopy to estimate the channel. Since the waves reflect, refract, diffract and scatter from the foliage, it is complicated to find the true travelling path between a transmitter and a receiver at the nodes. The AoA estimator is used for physical interpretation of the channel. The experimental results demonstrate the channels in a tree canopy are mostly matched with the General Extreme Value model. The measured path gains illustrate that the appropriate antenna patterns must be selected to enhance the reliability of the system.

1. INTRODUCTION

Wireless sensor network which sensor nodes monitor object and send the measured signals via sensor nodes to the master node to monitor, control, activate, etc.. It has played an important role in various applications, e.g., civilian, medical, agricultural, military, etc. [1–3]. In agricultural applications, it is essential in quality control of fruit production. For instance, a microwave sensor has been installed on Durian fruit [4] for monitoring ripeness. Then, signals corresponding to ripeness are sent from fruits on a tree to a tree node on such tree

Received 1 February 2013, Accepted 26 April 2013, Scheduled 6 March 2013

* Corresponding author: Monai Krairiksh (kkmonai@kmitl.ac.th).

and the master node, respectively, to warn growers to harvest at the appropriate time. In order to design the system to operate successfully with minimum power consumption to yield the longest operation time, channel characteristics of wireless communications in a tree canopy is desirable. The information of path loss exponent, including antenna installation is necessary.

A number of channel models for wireless communications through the trees have been conducted, either theoretically [5–8] or experimentally. The theoretical models have the advantage that it is not necessary to setup experiment but it needs computation intensive and is difficult to model since the channel is random. The experimental model requires a large number of experiments but it can provide information of the real situation. For experimental investigations, fading of radio channel at 800/900 MHz through moderately dense foliage were measured [9]. Propagation losses due to foliage at various frequencies that enabled one to know margin in reliable system design and cost effective deployment was investigated [10]. Effect of tree motions that found uncertainty accounted with the predicted coverage was investigated in [11]. Radio channel at various frequencies from 2 GHz to 60 GHz was measured and found that distributions at different frequencies are different due to different electrical size of leaves and branches [12]. This work is important to the design of smart receiver/transmitter that compensates or pause the data transmission when the fade is detected.

For environmental effects, effects of wind on scattering from vegetation at cellular phone frequencies and on line-of-sight channel obstructed by foliage have been investigated in [13, 14], respectively. Large and rapid signal fading occur from tree motions and high gain directive antennas were recommended to mitigate multipath fading. Signal propagated through two different tree shapes and sizes were measured [15]. By taking effect of wind into account, signal variation varies corresponding to wind speed and period of fading can be predicted by second-order statistical analysis. The effects of rain investigated in [16] exhibits significant attenuation at frequency higher than 5 GHz. It was shown that dominant component resulting from lateral waves is not affected by the rainy weather conditions. The accumulation of the rain water on the scatters such as the randomly distributed leaves, branches and tree trunks in the forest, produces a significant multipath component.

Signal strength at 240 MHz and 700 MHz through palm trees was measured to establish a channel model [17]. The Rician distribution was used to interpret the physical meaning and estimate the line-of-sight and non-line-of-sight components. They described the Rician

k-factor decreases as the strength of either wind or rain increases for high frequencies due to motion of branches and leaves. Furthermore, the k-factor at 700 MHz is less than that of 240 MHz due to different electrical size of branches and leaves. The work that comprehensively reviewed of channel through trees at microwave to millimeter waves published in [18] summarized that wet foliage produces about 6–8 dB attenuation/meter over the dry foliage that produces about 2–4 dB/meter.

Since, Tx-Rx modules are utilized for both sensing ripeness of fruit and communications, the low frequency has the large antenna size which may be larger than the size of the fruit. Therefore, the frequencies of operation are 2.45 GHz and 5.2 GHz, the ISM band whose is license free and a number of RF modules are available in the market. Although there are a number of works related to effect of vegetation on propagation channel as aforementioned and in [19–22], most of them are focused on propagation channel through the tree canopies. There is a lack of knowledge for propagation in a tree canopy. Therefore, the aim of this work is to investigate the wireless communication channel in a tree canopy which will be used for designing wireless communications between sensor nodes attached to fruits to monitor ripeness and send the information to the node installed beneath the tree. The research on UHF wireless communications in a tree canopy has been conducted [23]. However, information at microwave frequencies has not been presented. Hence, this work performs channel measurement in a tree canopy at 2.45 and 5.2 GHz using angle of arrival estimation, the probability density function (PDF) and the path loss.

This paper is organized as follow. Section 2 describes a measurement campaign and a dual-band phased array of switched-beam elements that will be utilized for angle-of-arrival (AOA) estimation. It will be used to interpret the physical behavior of the channel. Section 3 describes the channel characteristics including probability distribution function of the signal and path loss. Section 4 recommends the suitable system based on the results obtained from the previous sections and conclusion will be in Section 5.

2. MEASUREMENT CAMPAIGN AND PHYSICAL INTERPRETATION

The measurements were performed in Nonthaburi, Thailand over a period of 3 weeks in April 2011 when it was summer in Thailand. The foliage chosen for this study is mango tree [*Mangifera indica*] over a flat terrain as a photograph shown in Fig. 1(a). The geometry of the

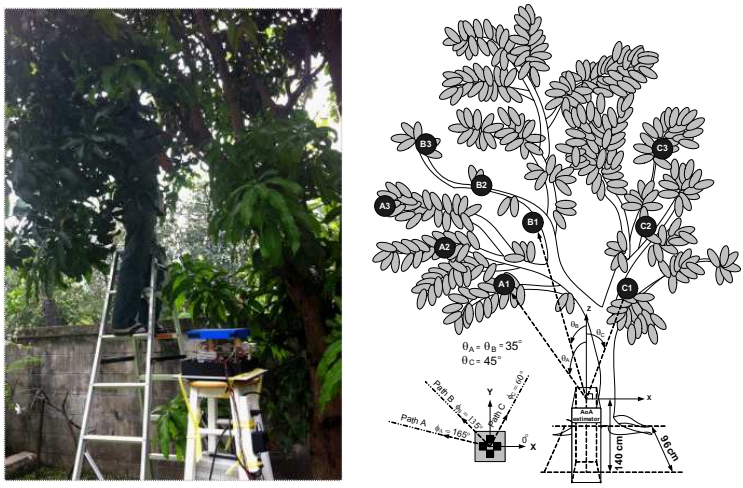

(a) (b)

Figure 1. Tree structure: (a) Photograph, (b) geometry.

problem of interest is shown in Fig. 1(b). The terrain mainly consists of soil and grass. The mango tree is approximately 5.2 m in height. The average tree trunk diameter is around 20 cm.

The measurements were carried out by using continuous-wave transmission at 2.45 GHz and 5.2 GHz. The quarter-wave monopole and half-wave patch antennas with a typical gain of 2.15 dBi and 4 dBi, respectively, were used for transmission at both frequencies. They were connected with a transmission line that was connected to a signal generator. The antennas were fastened at the branches of the tree. The positions of transmitting antennas were changed whereas the receiving antenna was fixed at the height of 1.4 m. The signal was transmitted from an Agilent N5182A signal generator through a 20 dB amplifier before being fed into the transmitting antenna. At a receiver, the AoA estimator was used for estimating the angle of arrived signal at both frequencies. An Agilent E4403B spectrum analyzer was used for measuring the received power at 2.45 GHz with an amplifier of 20 dB gain. At the frequency of 5.2 GHz, an Agilent 8592L spectrum analyzer was used for measuring the received power with 20 dB gain amplifier. Measurement paths were divided to three conditions. Environment of each path was different depending on a number of foliage and branch that directly affect the characteristics of the channel. The detail of each condition is described as follow.

Path A is the non-line-of-sight channel. The wave from the

transmitter cannot propagate directly to the receiver because it was covered by foliage. The distance from positions A1, A2, and A3 to the receiver are 1.6, 2.2, and 2.8 m, respectively. The angle θ_A with respect to z axis is 35°, and angle ϕ_A with respect to x axis is 165°.

Path B is the line-of-sight channel where the wave from the transmitter can propagate to the receiver without obstacle. Some part of the path was slightly blocked by foliage and a few small branches. The distance from positions B1, B2, and B3 to the receiver are 1.5, 2, and 2.4 m, respectively. The angle θ_B with respect to z axis is 45°, and angle ϕ_B with respect to x axis is 135°.

Path C is the non-line of sight channel. The wave from the transmitter cannot propagate directly to the receiver because it was covered by foliage, big branches, and small bunches. The distance from positions C1, C2, and C3 to the receiver are 1.2, 1.9, and 2.7 m, respectively. The angle θ_c with respect to z axisis 45° and angle ϕ_c with respect to y axis is 6°.

A dual-band AoA estimator consists of three main parts, i.e., receiver, interface, and display. The receiver utilizes a dual-band phased array of switched beam elements having four dual band patch antennas arranged as a circular array. The phase shifters for feeding each element are fixed at ±95.5° to cover a beam in two quadrants in front of the antenna. By changing the feed probe position at each element, radiation patterns of the array can be switched. The RF power detector transforms the received power to D.C. signal and is delivered to a microcontroller board. The ratio of the measured path gains is used to compare with the ratio of the patterns for the same beams. Knowing the region and the angle range of the region, the AOA can be obtained by finding the smallest difference between the measured maximum path gain ratio and the antenna pattern ratio for the corresponding region [24]. The detail of this AOA estimator is described in [25]. The RF signal is down converted to low frequency and converted to digital signal. A P89V51RD2 microcontroller was used for controlling antenna patterns and interfacing the receiver with the display on a personal digital assistance (PDA). The accuracy of this AOA estimated is ±5°. It should be noted that AOA estimations were calibrated for the elevation angle of 45°. Measurement in other directions may cause an error.

The AOA were estimated for 1500 times at each position; A1, B1, and C1, see Fig. 2(a). The AOA for 2.45 GHz and 5.2 GHz are plotted in Fig. 2(b) and Fig. 2(c), respectively. In each figure, the corresponding AOA for positions A1, B1 and C1 are shown. The black lines show direction and field strength whereas the figures in the parentheses illustrate the number of occurrence in such direction.

The field strength is plotted from the average value of field strength obtained from the number of occurrence in such direction. All the field strength in Figs. 2(b) and (c) are normalized to the same reference value. For illustration, Fig. 2(b) at position A1 shows that the strongest signal is in the direction 170° where there are four multipath signals in directions 158°, 150°, 135°, and 107°, respectively. The number of occurrences in the corresponding directions is 859, 312, 108, 96 and 101, respectively.

Obviously, (for case A1) the direct wave arrives at the AOA

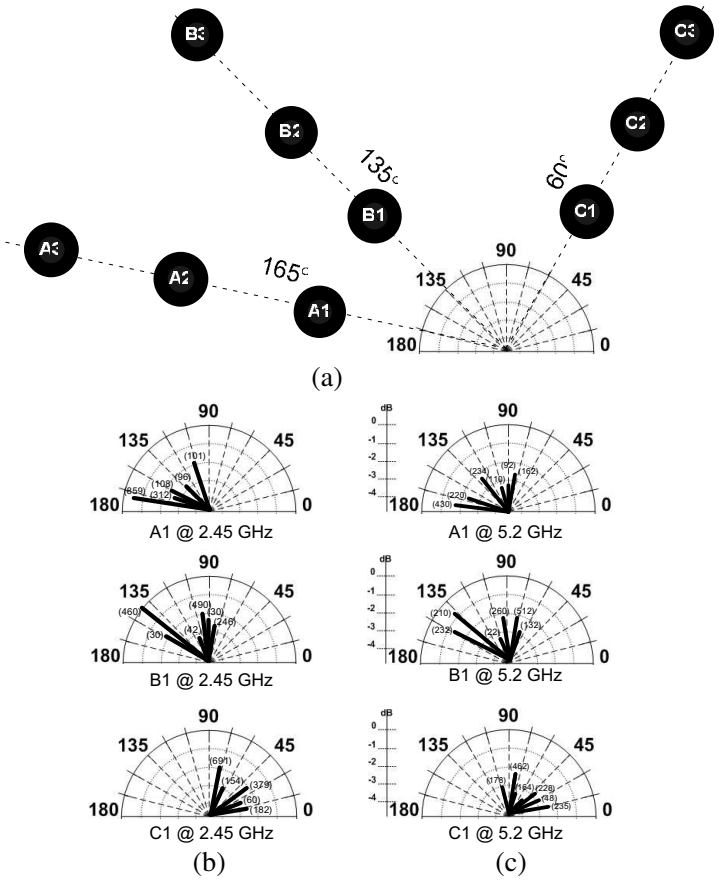

Figure 2. AoA estimations for positions A1, B1 and C1: (a) Geometry, (b) for 2.45 GHz, (c) for 5.2 GHz. (Numbers in parentheses are the number of occurrences and the field strength is normalized to the maximum level).

estimator at the angle 170°, as in Fig. 2(b). Since A1 is the nearest position, the field strength is strong. Fig. 2(b) (for position B1) shows that there are multi-paths from position B1 to AOA estimator, e.g., in the directions 148°, 107°, 96°, 90° and 80°. The direct path is at 138°. The AOA estimator received signal from many paths since the transmitting antenna is an omnidirectional antenna. Note that at the angles between 150°–180°, the AOA estimator cannot receive the signal since there are many leaves along the path for 2.45 GHz. At this frequency, the wavelength is about 12 cm which is comparable to the size of the leaves. Most of the wave energy is absorbed in the leaves. Also at the angles 0°–80° energy is attenuated since it is scattered from the leaves and branches.

According to Fig. 2(a), the nearest direct path of C1 should be 60° but due to diffracting and scattering from a big branch along the path, the strongest signals in Fig. 2(b) are in directions 79° and 40°, respectively. In addition, the field strength is markedly reduced due to attenuation in leaves and the received signal is scattered wave from the branch. Note that AOA for A2, B2 and C2 are similar to those of A1, B1 and C1 in the corresponding paths. However, those for positions A3, B3 and C3 are different due to the longer distances posses more multipath components.

For 5.2 GHz, the wavelength is about 5.8 cm and the length of leaf is about two wavelengths. Hence, the AOA estimator received signal from many directions. The signals arrives the AOA estimator in Fig. 2(c) (for position A1) in the directions of 170°, 160°, and 130°, 105°, 90° and 80° according to the wave scattered from the leaves and branches. For position B1, the possible direct wave is in direction 140° whereas the AOA estimator received waves from the directions 148°, 120°, 100°, 80° and 75°. The position C1 does not have strong direct wave since the transmitter was installed behind the branch. Therefore, there are many diffracted waves from directions 105°, 82°, 74°, 42°, 29° and 13°.

It is evident that the channel in a tree canopy is a multipath channel. At both frequencies, there is a direct path signal and many multipath signals. Since the leaves can be represented as thin discs [26], electrical dimensions of leaves and branches at 5.2 GHz are larger than those of 2.45 GHz, resulting in more scattered waves and hence multipath signals. Although the General Extreme Value function gives the best fit to the measured data, the channels for both frequencies possess multipath signals which generally can be explained by Rician function. Therefore, the Rician channel which Rician factor (k-factor) is a ratio of power in direct path to power in multipaths [27] will be discussed. From the measured results, the k-factors for 2.45 GHz and

5.2 GHz can be estimated as listed in Table 1 in Section 3. The physical behavior of the channel can be interpreted simply by using the AOA estimation. The accurate k-factor will be elaborated in Section 3.

3. CHANNEL CHARACTERIZATION

In wireless communication, signal arrives the receiving antenna consists of direct and multipath signals reflecting, scattering and diffracting from environments. These result in fading of signal when they are destructively combined with the direct signal. Channel can be characterized statistically where generally it can be divided into line-of-sight and non-line-of-sight channels. The typical channels are Rician, Rayleigh, Nakagami, Lognormal [15, 17]. However, some functions are used to represent channel through foliage, e.g., General Extreme Value, Inverse Gaussian, Weibull [12]. From the procedure described in Section 2, signal along path A at positions A1, A2 and A3; path B at positions B1, B2 and B3; and path C at positions C1, C2 and C3 were measured at 2.45 GHz and 5.2 GHz. Two thousand samples were measured in each condition then the PDF, normalized to mean voltage for each position, were plotted in Fig. 3 for 2.45 GHz and in Fig. 4 for 5.2 GHz. The PDF in Fig. 3(a) and Fig. 3(b) corresponding to path A and path B are plotted with the General Extreme Value, Lognormal, Inverse Gaussian and Weibull functions. Fig. 3(c) shows PDF of the

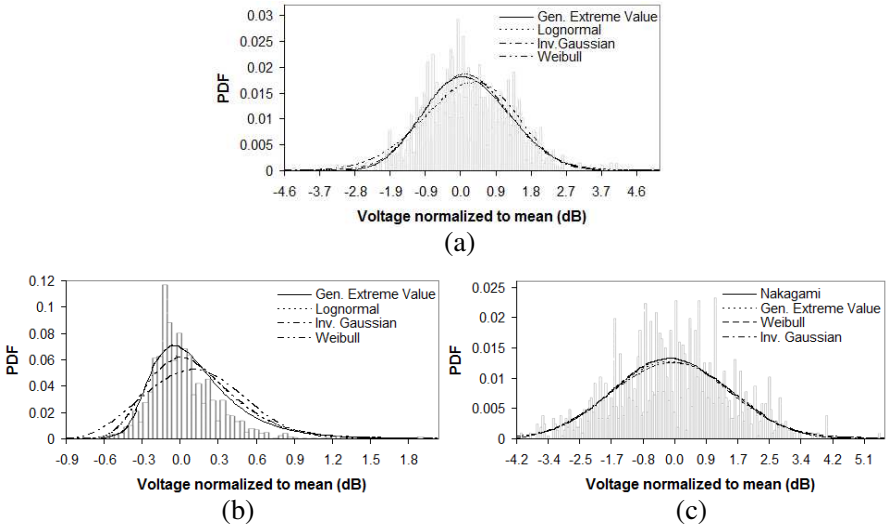

Figure 3. PDF for 2.45 GHz: (a) Path A, (b) path B, (c) path C.

signal on path C which the Nakagami, General Extreme Value, Weibull and Inverse Gaussian functions are plotted on the same graph. We plotted these functions since they provided the best match with the measured PDF. The error can be estimated by the root mean square error (Erms) between sampled PDF with the known functions [17].

For the results of 5.2 GHz in Fig. 4, General Extreme Value, Nakagami, Inverse Gaussian and Lognormal functions are plotted with the sampled PDF. The Erms are listed in Table 2. For 2.45 GHz; Lognormal, General Extreme Value and General Extreme Value provide the best fit to the sampled PDF in path A, path B and path C, respectively. For 5.2 GHz, General Extreme Value is the best fit to sampled PDF in path A and B whereas path C is Lognormal. We used these functions to model the channels in different situations and frequencies. Note that Rician distribution has slightly higher Erms, but it is convenient to describe behavior of the channel. The k-factors for both frequencies at the mentioned paths are listed in Table 1. The k-factors of path B are highest due to no obstacle along the path. Path C has the lowest k-factor since there is a branch between the transmitting and receiving antennas. Those for 5.2 GHz have lower k-factors due to electrical size of leaves and branches are larger than those at 2.45 GHz. This information essentially supports the physical interpretation in Section 2. In addition, these PDF models will be used to calculate cumulative distribution function (CDF) that represents the

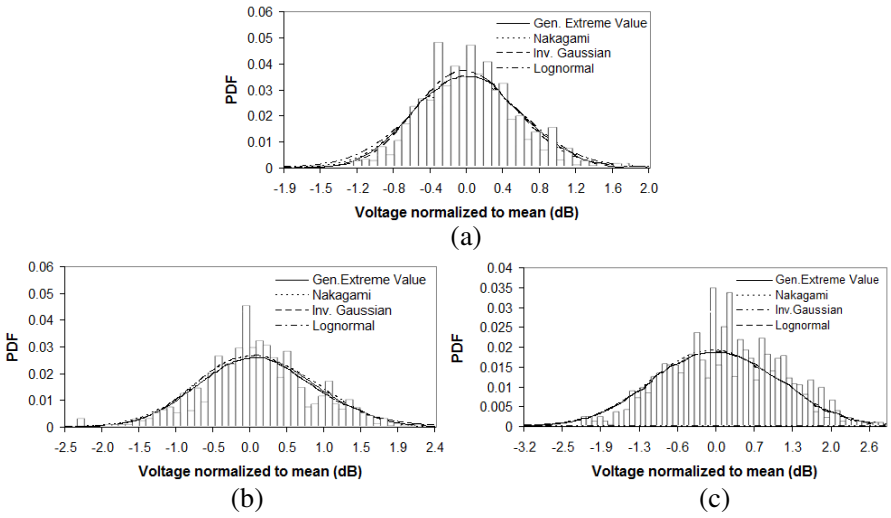

Figure 4. PDF for 5.2 GHz: (a) Path A, (b) path B, (c) path C.

Table 1. k-factors for different paths from AoA estimator and PDF data.

Path \ Frequency	2.45 GHz		5.2 GHz	
	AoA Est. (dB)	PDF (dB)	AoA Est. (dB)	PDF (dB)
A	6.14	7.65	4.21	5.45
B	9.12	11.26	5.25	6.42
C	4.62	5.23	2.54	3.25

Table 2. Average E_{RMS} for each distribution.

Model	**E_{RMS}**			
	Path A		Path B	
	2.45 GHz	5.20 GHz	2.45 GHz	5.20 GHz
Gen.Ext.Value	0.09	0.07	0.05	0.03
Inv.Gaussian	0.13	0.08	0.05	0.04
Lognormal	0.07	0.09	0.06	0.51
Weibull	0.12	0.09	0.11	0.57
Rician	0.14	0.13	0.11	0.09
Rayleigh	0.15	0.38	0.13	0.43
Nakagami	*Not fit*	0.08	0.13	0.03
Model	**E_{EMS}**			
	Path C			
	2.45 GHz	5.20 GHz		
Gen.Ext.Value	0.04	0.03		
Inv.Gaussian	0.28	0.02		
Lognormal	0.15	0.02		
Weibull	0.08	0.06		
Rician	0.14	0.06		
Rayleigh	0.10	0.40		
Nakagami	0.11	0.03		

probability the signal being less than the specified level that will be used for estimating reliability of the wireless communication system.

It is noted that k-factors obtained from the AOA estimator have lower values than those from PDF data since they were estimated from the ratio of power in direct path to power in multipath. Nevertheless, it clearly interprets physical behavior of the channels.

To design the link budget, the path loss along with transmitter

and receiver parameters must be known. To evaluate path loss, a setup in Fig. 5 was set. Signal levels at three positions along path A, B and C at both frequencies were measured. Then, they were converted to path loss using Equation (1). The path loss at 2.45 GHz and 5.2 GHz are illustrated in Figs. 6(a) and (b), respectively.

$$\text{Path loss} = \frac{P_T G_{AT} G_T G_R G_{AR}}{L_{TX} L_{RX} P_R} \tag{1}$$

where P_T is transmit power (0 dBm); G_{AT} and G_{AR} are transmit and receive amplifier gain (20 dB); G_T and G_R are transmit and receive antenna gain (2.15 dBi); L_{TX} and L_{RX} are transmit and receive cable loss (5 dB); P_R is receive power.

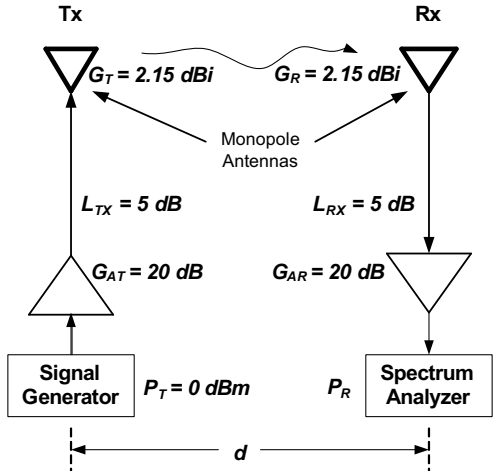

Figure 5. Path loss measurement setup.

The path loss exponents at 2.45 GHz for the path A, B and C in Fig. 6(a) are −8.5, −3.5 and −3.5, respectively, whereas the corresponding path loss exponents for 5.2 GHz in Fig. 6(b) are −16, −5 and −4.5, respectively. The higher frequency of 5.2 GHz possesses higher path loss than the lower frequency of 2.45 GHz since attenuation in leaves is higher than at 2.45 GHz. In addition, the scattered waves from leaves contribute to multipath components. Consequently, k-factor in path A is lower than the other paths. However, comparing between 2.45 GHz and 5.2 GHz, the former possesses higher k-factor due to less power of scattered components than the former one. For path B and C, path loss is lower than path A due to less density of leaves. Path loss has dominant effect from the stem and branches. It is relevant that 5.2 GHz has higher loss than 2.45 GHz.

The effects of trunk (path B) and branches (path C) for 2.45 GHz in Fig. 6(a) contribute to path loss exponents in the order of 3.5 which is comparable to the value in the range of 2.48–3.60 existing in literature [20]. However, 5.2 GHz in Fig. 6(b) possesses higher path loss exponent than for 2.45 GHz due to the larger electrical size of branches and trunk. Hence, the higher attenuation and scattered wave are obtained. The obtained results are higher than those from literature (at 5.8 GHz) of 3.3 to 3.6 [28]. The differences are attributed from the different trees, different frequencies and different environments since this work installed a transmitter in a tree canopy.

This information can be used to design the transmitting power once the distance in each situation, sensitivity of receiver, gains of the antennas used, are specified. However, reliability of the system will be ensured when the CDF of the signal from the models are estimated.

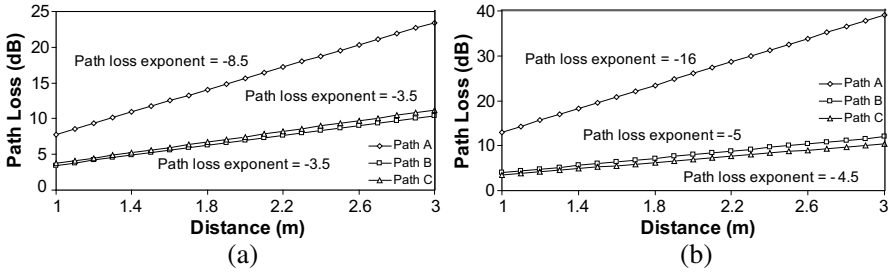

Figure 6. Path loss of each frequency: (a) 2.45 GHz, (b) 5.2 GHz.

4. SYSTEM DESIGN

Since the sensor nodes must be small for installing with a fruit, the antenna size is limited, and consequently gain is low. However, using an omnidirectional antenna like a monopole antenna has a possibility to transmit signal in many directions. Microstrip antenna, possessing small size and light weight, has directional pattern that can mitigate multipath signal better than the monopole antenna. In this section, effect of antenna pattern on performance of the system in various channels will be discussed. A microstrip antenna was installed at the same position with the monopole antenna to transmit signal for 2,000 samples and the CDF curves were plotted. Fig. 7 shows the results for 2.45 GHz whereas Fig. 8 shows those for 5.2 GHz. Let consider Fig. 7(a) in which path A consists of many leaves. Thus, Rician channel having moderate k-factor of 7.65 dB is used. The path gain was measured by taking the difference between the monopole antenna and the microstrip

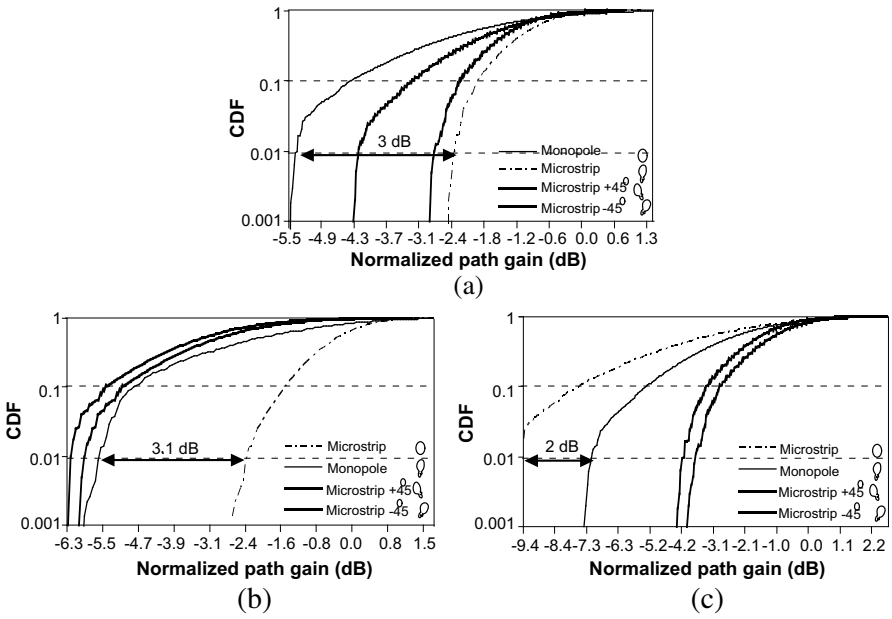

Figure 7. Comparison of CDF between monopole and microstrip antennas at 2.45 GHz: (a) Path A, (b) path B, (c) path C.

antenna at the outage of 1%. Using directional antenna provides better performance than the omnidirectional antenna, i.e., higher path gain of around 3 dB with reliability of 99% when a microstrip antenna was installed to have main beam directed to the receiver. The path gain reduced 1.3 dB and 2.7 dB when the main beam of the microstrip antenna was shifted by $+45°$ and $-45°$, respectively. In this case, installing to have main beam in line with the direction of the receiver provided the best performance.

For path B in Fig. 7(b) which is the line-of-sight condition, the highest k-factor of 11.26 dB the directional antenna provided higher path gain than the monopole antenna counterpart by 3.1 dB. However, when the main beam was shifted by $\pm 45°$, path gain of the microstrip antenna was lower than that of the monopole antenna. Hence, the microstrip antenna has to be installed to have maximum of the pattern directed to the receiver. In the situation of path C in Fig. 7(c), there is a branch and there are many leaves on the way between the transmitter and the receiver. The signals arrived the receiver are the scattered signals from the branch and the leaves. Therefore, using the microstrip antenna to receive the direct wave is not suitable and the path gain is

less than that of the monopole antenna by about 2 dB. Nevertheless, when the main beam of the microstrip antenna was shifted by ±45°, path gain is higher than that the monopole antenna by about 3 dB. The behavior of path gain for 5.2 GHz, in general are similar to those for the 2.45 GHz. Path gain in path A and B are achieved when a microstrip antenna is used whereas monopole antenna provided higher path gain than microstrip antenna counterpart in path C. However, the quantity is different as shown in Fig. 8. Consequently, suitable antenna installation must be considered in a specific path. From the above results, we may conclude that the microstrip antenna is suitable for this application. In general, it will be installed to direct the main beam to the receiver. For the non-line-of-sight case, it should be installed so that main beam is shifted by possibly be ±45°.

In the system design, antenna pattern and sensitivity of the receiver must be known. Path losses in Fig. 6 are used to calculate basically how much power will be transmitted for each specific node. Then, channel models suitable for the specific path will be selected to plot CDF curves to find reliability of the system when margin from environmental effects are taken into account. Finally, suitable antenna

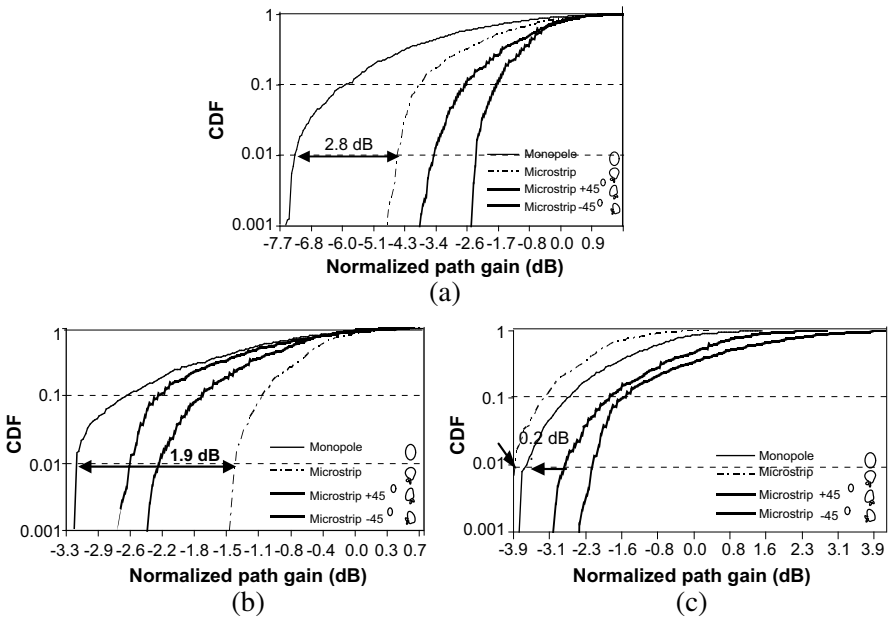

Figure 8. Comparison of CDF between monopole and microstrip antennas at 5.2 GHz: (a) Path A, (b) path B, (c) path C.

pattern installation at a specific node must be concerned. Typically, the main beam of the antenna is installed to point to the transmitter except the case there are branches on the way between the transmitter and the receiver, the antenna pattern must be slightly shifted. From these considerations, a reliable wireless communication system in a tree canopy can be accomplished.

5. CONCLUSIONS

From the desirable of wireless communications in a tree canopy, this work investigated channel models on a mango tree which represented a tree with moderate leave and branch size. Measurements of path loss and field distribution at 2.45 GHz and 5.2 GHz were performed. By cutting branches and leaves, three types of channel, i.e., leaves are majority, branches are majority, and combination of leaves and branches, are presented. Angle of arrival of signals can clearly interpret physical behavior of the channels. PDF curves were plotted to match with the known distribution functions. It was found that mostly General Extreme Value had the best matched at 2.45 GHz and 5.2 GHz. Physical interpretation whether the channel be either line-of-sight or non-line-of-sight, Rician distribution was utilized incorporated with angle of arrival estimation. The results from this work enable one to design a reliable wireless communication system in a tree canopy that is essential in fruit pre-harvesting control.

ACKNOWLEDGMENT

The authors gratefully appreciate the anonymous reviewers for valuable comments that significantly improve the manuscript. This work was supported by the Telecommunications Research and Industrial Development Institute, National Broadcasting and Telecommunications Commission Fund (Grant No. PHD002/2551) and the Thailand Research Fund (TRF) under the senior research scholar project (Grant No. RTA-518002).

REFERENCES

1. Akyildiz, F., W. Su, Y. Sankarasubramaniam, and E. Cayirci, "Wireless sensor network: Survey," *Computer Network*, Vol. 38, 393–422, 2002.
2. Ochiai, H., H. Ishizuka, Y. Kawakami, and H. Esaki, "A DTN-based sensor data gathering for agricultural applications," *IEEE Sensor Journal*, Vol. 11, No. 11, 2861–2868, Nov. 2011.

3. Alejos, A. V., M. G. Sánchez, I. Cuiñas, and J. C. G. Valladares, "Sensor area network for active RTLS in RFID tracking applications at 2.4 GHz," *Progress In Electromagnetics Research,* Vol. 110, 43–58, 2010.
4. Krairiksh, M., J. Varith, and A. Kanjanavapastit, "Wireless sensor network for monitoring maturity stage of fruit," *Science Research/Wireless Sensor Network*, Vol. 3, 318–321, 2011.
5. De Jong, Y. L. C. and M. H. A. Herben, "A tree-scattering model for improved propagation prediction in urban microcells," *IEEE Trans. on Vehicular Technology,* Vol. 53, No. 2, 503–513, Mar. 2004.
6. Chee, K. L., S. A. Torrico, and T. Kurner, "Foliage attenuation over mixed terrains in rural areas for broadband wireless access at 3.5 GHz," *IEEE Trans. on Antennas and Propagation*, Vol. 59, No. 7, 2698–2706, Jul. 2011.
7. Au, W. C., L. Tsang, R. T. Shin, and J. A. Kong, "Collective scattering and absorption effects in microwave interaction with vegetation canopies," *Progress In Electromagnetics Research,* Vol. 14, 181–23, 1996.
8. De Matthaeis, P. and R. H. Lang, "Microwave scattering models for cylindrical vegetation components," *Progress In Electromagnetics Research,* Vol. 55, 307–333, 2005.
9. Bultitude, R. J. C., "Measured characteristics of 800/900 MHz fading radio channels with high angle propagation through moderately dense foliage," *IEEE Journal on Selected Areas in Communications*, Vol. 5, No. 2, 116–127, Feb. 1987.
10. Dalley, J. E. J., M. S. Smith, and D. N. Adams, "Propagation losses due to foliage at various frequencies," *National Conference on Antennas and Propagation Publication*, No. 461, 267–270, Mar.–Apr. 1999.
11. Lewenz, R., "Path loss variation due to vegetation movement," *National Conference on Antennas and Propagation Publication,* No. 461, 97–100, Mar.–Apr. 1999.
12. Perras, S. and L. Bouchard, "Fading characteristics of RF signals due to foliage in frequency bands from 2 to 60 GHz," *Proc. 5th Int. Symp. Wireless Personal Multimedia Commun.,* 267–271, Honolulu, Hawai, Oct. 2002.
13. Cuiñas, I., A. V. Alejos, M. G. Sánchez, P. Gómez, and R. F. S. Caldeirinha, "Wind effect on the scattering from vegetation at cellular phone frequencies," *Proc. of International Geoscience and Remote Sensing Symposium*, 369–372, 2007.

14. Pelet, E. R., J. E. Salt, and G. Wells, "Effect of wind on foliage obstructed line of-sight channel at 2.5 GHz," *IEEE Trans. on Broadcasting,* Vol. 50, No. 3, 224–232, Sep. 2004.
15. Hashim, M. H. and S. Starou, "Measurements and modeling of wind influence on radiowave propagation through vegetation," *IEEE Trans. on Wireless Communications,* Vol. 5, No. 5, 1055–1064, May 2006.
16. Meng, Y. S., Y. H. Lee, and B. H. Ng, "Investigation of rainfall effect on forested radio wave propagation," *IEEE Trans. on Antennas and Wireless Propagation Letters,* Vol. 7, 159–162, 2008.
17. Meng, Y. S., Y. H. Lee, and B. C. Ng, "The effects of tropical weather on radio-wave propagation over foliage channel," *IEEE Trans. on Vehicular Technology,* Vol. 58, No. 8, 4023–4030, Oct. 2009.
18. Meng, Y. S. and Y. H. Lee, "Investigations of foliage effect on modern wireless communication systems: A review," *Progress In Electromagnetics Research,* Vol. 105, 313–332, 2010.
19. Blaunstein, N., D. Censor, D. Katz, A. Freedman, and I. Matityahu, "Radio propagation in rural residential areas with vegetation," *Progress In Electromagnetics Research,* Vol. 40, 131–153, 2003.
20. Gay-Fernández, J. A., M. G. Sánchez, I. Cuiñas, A. V. Alejos, J. G. Sánchez, and J. L. Milanda-Sierra, "Propagation analysis and deployment of a wireless sensor network in a forest," *Progress In Electromagnetics Research,* Vol. 106, 121–145, 2010
21. Alejos, A. V., M. Dawood, and L. Medina, "Experimental dynamical evolution of the Brillouin precursor for broadband wireless communication through vegetation," *Progress In Electromagnetics Research,* Vol. 111, 291–309, 2011
22. Morgadinho, S., R. F. S. Caldeirinha, M. O. Al-Nuaimi, I. Cuiñas, M. C. Sancház, T. R. Fernandes, and J. Richter, "Time-variant radio channel characterization and modelling of vegetation media at millimeter-wave frequency," *IEEE Trans. on Antennas and Propagation,* Vol. 60, No. 3, 1557–1568, Mar. 2012.
23. Sooksumrarn, P. and M. Krairiksh, "UHF wireless communication channel in a tree canopy," *Proc. of International Symposium on Antennas and Propagation*, 311–314, Oct.–Nov. 2012.
24. Kamarudin, M. R., Y. I. Nechayev, and P. S. Hall, "Onbody diversity and angle-of-arrival measurement using a pattern switching antenna," *IEEE Trans. on Antennas and Propagation,* Vol. 57, No. 4, 964–971, Apr. 2009.

25. Sooksumrarn, P. and M. Krairiksh, "Dual-band mobile angle of arrival estimator," *Proc. of Asia-Pacific Microwave Conference,* 729–732, Dec. 2010.
26. Torrico, S. A. and R. H. Lang, "A simplified analytical model to predict the specific attenuation of a tree canopy," *IEEE Trans. on Vehicular Technology,* Vol. 56, No. 2, 696–703, Mar. 2007.
27. Saunders, S. R. and A. A. Zavala, *Antennas and Propagation for Wireless Communication Systems*, 2nd Edition, John Wiley, 2007.
28. Cuiñas, I., J. A. Gay-Fernández, P. Gómez, A. V. Alejos, and M. G. Sánchez, "Radioelectric propagation in mature wet forests at 5.8 GHz," *Proc. of IEEE International Symposium on Antennas and Propagation Society,* 2009.